

A high-quality-factor ultra-narrowband perfect metamaterial absorber based on monolayer molybdenum disulfide

Liying Jiang(蒋黎英), Yingting Yi(易颖婷), Yijun Tang(唐轶峻), Zhiyou Li(李治友),Zao Yi(易早), Li Liu(刘莉), Xifang Chen(陈喜芳), Ronghua Jian(简荣华),Pinghui Wu(吴平辉), and Peiguang Yan(闫培光)

Citation: Chin. Phys. B, 2022, 31 (**3**): 038101. DOI: 10.1088/1674-1056/ac1e11
Journal homepage: http://cpb.iphy.ac.cn; http://iopscience.iop.org/cpb

What follows is a list of articles you may be interested in

A multi-band and polarization-independent perfect absorber based on Dirac semimetals circles and semi-ellipses array

Zhiyou Li(李治友), Yingting Yi(易颖婷), Danyang Xu(徐丹阳), Hua Yang(杨华), Zao Yi(易早), Xifang Chen(陈喜芳), Yougen Yi(易有根), Jianguo Zhang(张建国), and Pinghui Wu(吴平辉)

Chin. Phys. B, 2021, 30 (**9**): 098102. DOI: 10.1088/1674-1056/abfb57

Dynamically tunable terahertz passband filter based on metamaterials integrated with a graphene middle layer

MaoSheng Yang(杨茂生), LanJu Liang(梁兰菊), DeQuan Wei(韦德泉), Zhang Zhang(张璋), Xin Yan(闫昕), Meng Wang(王猛), JianQuan Yao(姚建铨)

Chin. Phys. B, 2018, 27 (**9**): 098101. DOI: 10.1088/1674-1056/27/9/098101

Robust stability characterizations of active metamaterials with non-Foster loads

Yi-Feng Fan(范逸风), Yong-Zhi Sun(孙永志)

Chin. Phys. B, 2018, 27 (**2**): 028102. DOI: 10.1088/1674-1056/27/2/028102

Polarization-insensitive unidirectional spoof surface plasmon polaritons coupling by gradient metasurface

Hong-yu Shi(施宏宇), An-xue Zhang(张安学), Jian-zhong Chen(陈建忠), Jia-fu Wang(王甲富), Song Xia(夏颂), Zhuo Xu(徐卓)

Chin. Phys. B, 2016, 25 (**7**): 078105. DOI: 10.1088/1674-1056/25/7/078105

Tri-band transparent cross-polarization converters using a chiral metasurface

Shi Hong-Yu, Li Jian-Xing, Zhang An-Xue, Wang Jia-Fu, Xu Zhuo

Chin. Phys. B, 2014, 23 (**11**): 118101. DOI: 10.1088/1674-1056/23/11/118101

A high-quality-factor ultra-narrowband perfect metamaterial absorber based on monolayer molybdenum disulfide

Liying Jiang(蒋黎英)[1,†], Yingting Yi(易颖婷)[2,†], Yijun Tang(唐轶峻)[3], Zhiyou Li(李治友)[1], Zao Yi(易早)[1,‡], Li Liu(刘莉)[1], Xifang Chen(陈喜芳)[1], Ronghua Jian(简荣华)[4], Pinghui Wu(吴平辉)[5,§], and Peiguang Yan(闫培光)[6]

[1] *Joint Laboratory for Extreme Conditions Matter Properties, Southwest University of Science and Technology, Mianyang* 621010, *China*
[2] *College of Physics and Electronics, Central South University, Changsha* 410083, *China*
[3] *College of Science, Zhejiang University of Technology, Hangzhou* 310023, *China*
[4] *School of Science, Huzhou University, Huzhou* 313000, *China*
[5] *College of Physics and Information Engineering, Quanzhou Normal University, Quanzhou* 362000, *China*
[6] *College of Physics and Optoelectronic Engineering, Shenzhen University, Shenzhen* 518060, *China*

(Received 8 May 2021; revised manuscript received 21 July 2021; accepted manuscript online 17 August 2021)

In order to significantly improve the absorption efficiency of monolayer molybdenum disulfide (M-MoS_2), an ultra-narrowband M-MoS_2 metamaterial absorber was obtained through theoretical analysis and numerical calculation using the finite difference time domain method. The physical mechanism can be better analyzed through critical coupling and guided mode resonance. Its absorption rate at $\lambda = 806.41$ nm is as high as 99.8%, which is more than 12 times that of bare M-MoS_2. From the simulation results, adjusting the geometric parameters of the structure can control the resonant wavelength range of the M-MoS_2. In addition, we also found that the maximum quality factor is 1256.8. The numerical result shows that the design provides new possibilities for ultra-narrowband M-MoS_2 perfect absorbers in the near-infrared spectrum. The results of this work indicate that the designed structure has excellent prospects for application in wavelength-selective photoluminescence and photodetection.

Keywords: metamaterials, ultra-narrowband, high quality factor, critical coupling

PACS: 81.05.Xj, 02.70.Bf, 33.20.Ea, 42.79.Ta **DOI:** 10.1088/1674-1056/ac1e11

1. Introduction

Metamaterials are manufactured materials designed to control the unique optical properties of electromagnetic waves. Much theoretical and experimental work on functional electromagnetic metamaterials has been carried since the first related work by Smith and colleagues.[1–3] In 2008, Landy *et al.*[4] successfully proved that perfect metamaterial absorbers can absorb nearly 100% of incident light in a wide wavelength range, and this discovery attracted much attention. So far, perfect metamaterial absorbers have been widely used in various fields, such as sensing,[5] imaging,[6] solar energy,[7] photodetectors,[8] photothermal conversion[9] and many more.

In recent years, graphene, which has good mechanical, electrical and optical properties, and transition metal disulfides (TMDCs) have received extensive attention.[10,11] Graphene absorbs only 2.3% of light due to its tapered electronic energy band structure.[12] Graphene optoelectronic devices also have metal attenuation and surface reflection factors which make it difficult to achieve high absorptivity. Unlike graphene, when transition metal binary compounds transform from a macroscopic structure to a two-dimensional (2D) monolayer structure they become direct band gap semiconductors. Of these, MoS_2 is the most typical monolayer transition metal disulfide, and its direct band gap is about 1.8 eV,[13] which has an important role in electronic transition. However, due to the inherent atomic thickness of MoS_2, it poses a great challenge at the weak light–matter interaction, and its extremely low light emission and absorption characteristics limit its application in the field of optoelectronic devices.[14] More specifically, monolayer MoS_2 with a thickness of 6–7 Å has an absorption rate as low as about 10% in the visible and near-infrared spectrum because of its unique electronic band structure.[15] Therefore, enhancing the light–matter interaction will greatly influence expansion of the range of application of optoelectronic devices based on 2D TMDCs.

In this work we use critical coupling and guided resonance to obtain a perfect absorber based on monolayer molybdenum disulfide (M-MoS_2), which realizes perfect absorption of the tunable ultra-narrow band of M-MoS_2. In addition, the change of the working wavelength and absorption efficiency of M-MoS_2 is closely related to the period of the structure and the thickness parameters of the dielectric layer. This adjustable and enhanced absorption peak of this structure has promising

[†]These authors contributed equally to this work.
[‡]Corresponding author. E-mail: yizaomy@swust.edu.cn
[§]Corresponding author. E-mail: phwu@zju.edu.cn

© 2022 Chinese Physical Society and IOP Publishing Ltd

applications in optoelectronic devices based on 2D TMDCs. At the same time, we also study the quality factor (Q-factor) and universality of the absorber and find that its Q-factor can be as high as 1256.8. The resonance device therefore provides a different potential direction for research and development for designing a TMDC tunable single-band M-MoS_2 perfect absorber.

2. Structure and design

M-MoS_2 is placed between a silicon dioxide (SiO_2) layer with a cross-shaped air channel structure and a two-dimensional polymethyl methacrylate (PMMA) layer (detailed models can be found in Figs. 1(a) and 1(b)). The bottom of the system comprises a silver layer (Ag) to act as a metal mirror, reducing light transmission and preventing the transmission of incident light. The medium in the cross-shaped air hole structure is set to air, and its refractive index is 1. The cross-shaped air hole is of equal height to the SiO_2 layer, represented by D_a and D_2, respectively, and the thickness of the PMMA layer and the Ag reflective layer is represented by D_4 and D_1, respectively. The periods of the absorber in the x and y directions are P_x and P_y, respectively.

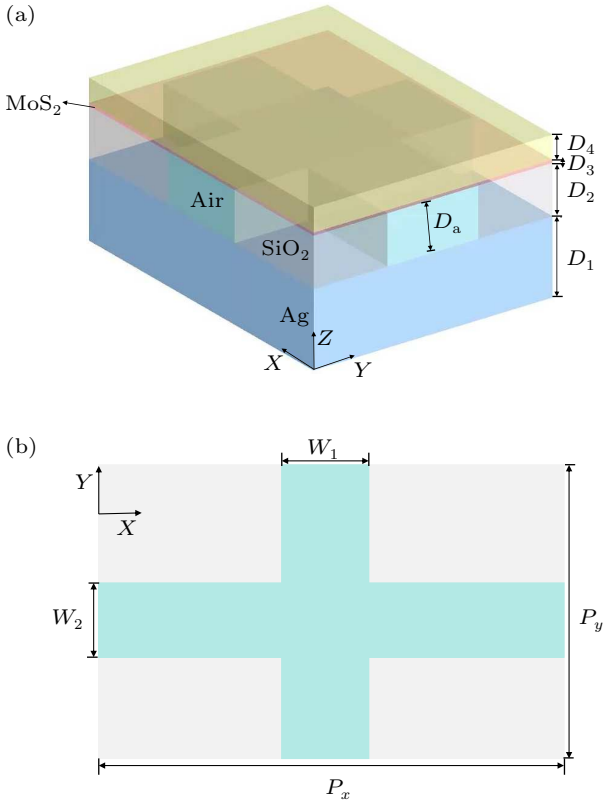


Fig. 1. (a) Three-dimensional schematic diagram of the M-MoS_2 absorption enhancement system. (b) Top view of a device with specified dimensions.

The cross-shaped air hole of the absorber is composed of two superimposed rectangular parallelepipeds. The widths of the two cuboids are W_1 and W_2, and the widths extending in the x and y directions are consistent with the period. The refractive indices of PMMA and SiO_2 are 1.48 and 1.45, respectively. The present invention takes the parameters when the absorber reaches the critical coupling state as the basic parameters for the entire performance analysis. Therefore, the basic parameters are as follows: PMMA layer thickness $D_4 = 35$ nm, depth of the cross-shaped air hole and SiO_2 layer thickness $D_a = D_2 = 180$ nm, thickness of the Ag reflective layer $D_1 = 275$ nm, width $W_1 = 100$ nm, width $W_2 = 90$ nm, period $P_x = 1020$ nm, period $P_y = 788$ nm. In the numerical calculation, the wavelength-dependent complex permittivity for MoS_2 ($D_3 = 0.615$ nm) studied by Li *et al.*[16] is used in our simulation. In this paper, we use the Drude model to express the complex permittivity of Ag as $\varepsilon_\infty = 3.7$, plasmon frequency $\omega_p = 1.38 \times 10^{16}$ s^{-1} and damping constant $\gamma = 2.73 \times 10^{13}$ s^{-1}.[17] The Drude model is[18]

$$\varepsilon(w) = \varepsilon_\infty - \frac{w_p^2}{(w^2 + i\gamma w)}. \tag{1}$$

In the simulation process, we select the normal incident light in the TM polarization mode (electric polarization parallel to the x-axis) and project it perpendicularly onto the structure, that is, $\theta = 0°$. Regarding the setting of the boundary conditions, periodic boundary conditions are selected parallel to the x and y directions and the perfectly matched layer is perpendicular to the z direction, i.e., PML boundary conditions.

3. Results and discussion

We have plotted the electric field ($|E|$) distributions of X–Y, X–Z, and Y–Z sections at 806.41 nm and 781 nm. Figures 2(a)–2(f) describe the transverse electric field diagrams of the same wavelength under resonance and non-resonance, respectively, and comparative analysis. Under critical coupling, the electric field strength near the M-MoS_2 increases greatly with cavity excitation,[19] but the absorber is not excited at this time. However, there is a difference: at the non-resonant wavelength of 781 nm, the electric field strength distribution near the M-MoS_2 layer is very weak. Meanwhile, the system develops over-coupling conditions. Compare the X–Y cross-sectional electric field at the resonant wavelength and the non-resonant wavelength, which is located above the structure. At the on-resonance wavelength of 806.41 nm, most of the electric field is distributed around the M-MoS_2 in the air hole, and the electromagnetic field at the air hole is almost completely absorbed by M-MoS_2 due to resonance. However, the electric field strength of the X–Y section at the off-resonant wavelength (781 nm) is not completely consumed due to the incident light field in the X-direction cavity, so the absorption strength of the structure in the on-resonant mode is obviously greater than that in the off-resonant mode. When the Y–Z electric field distribution is in resonance, the electric field is mainly on the left and right sides of the Y-axis, forming a standing

wave mode. The electric field diagram under off-resonant conditions shows that the overall strength is not high. Finally, the resonance and off-resonance modes in the X–Z direction also have the same characteristics.

It is well known that change in the period profoundly affects the frequency of the surface resonance mode of the metamaterial.[20–22] We will now explore the relationship between the absorption characteristics of the absorber in each

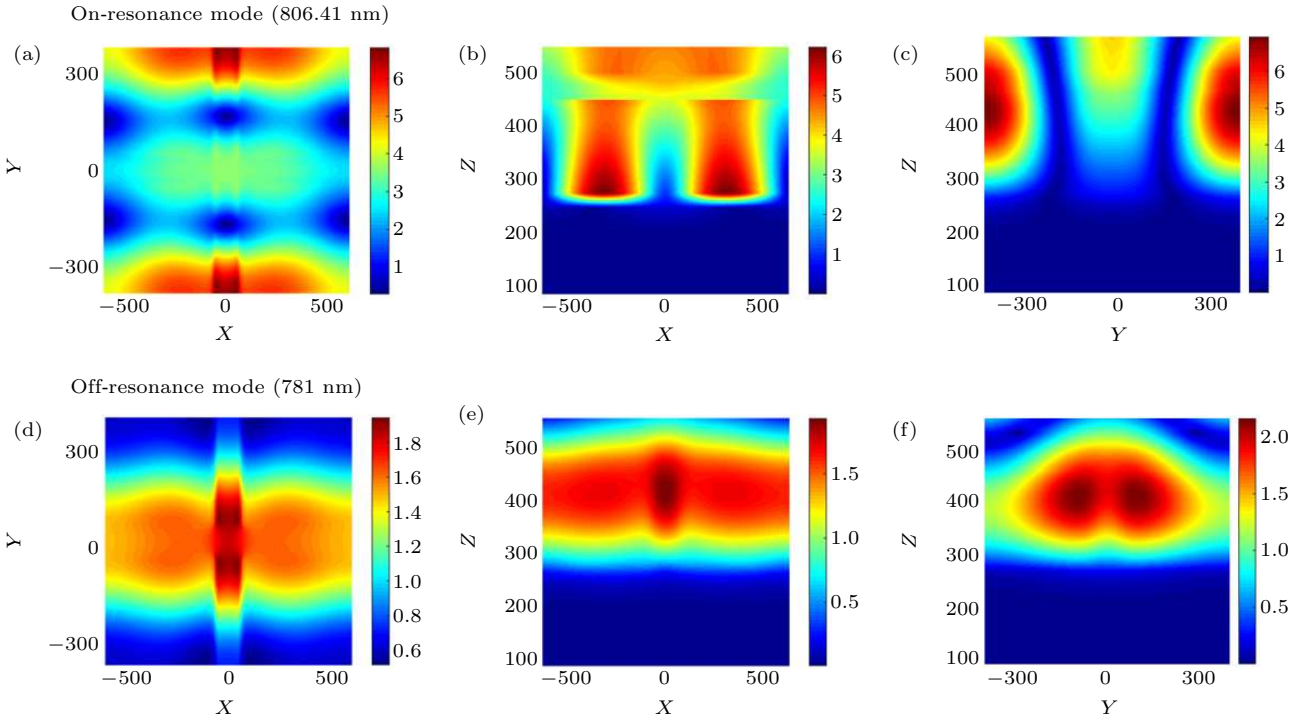


Fig. 2. (a)–(f) The electric field ($|E|$) distribution of X–Y, X–Z, and Y–Z sections at 806.41 nm (resonant wavelength) and 781 nm (non-resonant wavelength).

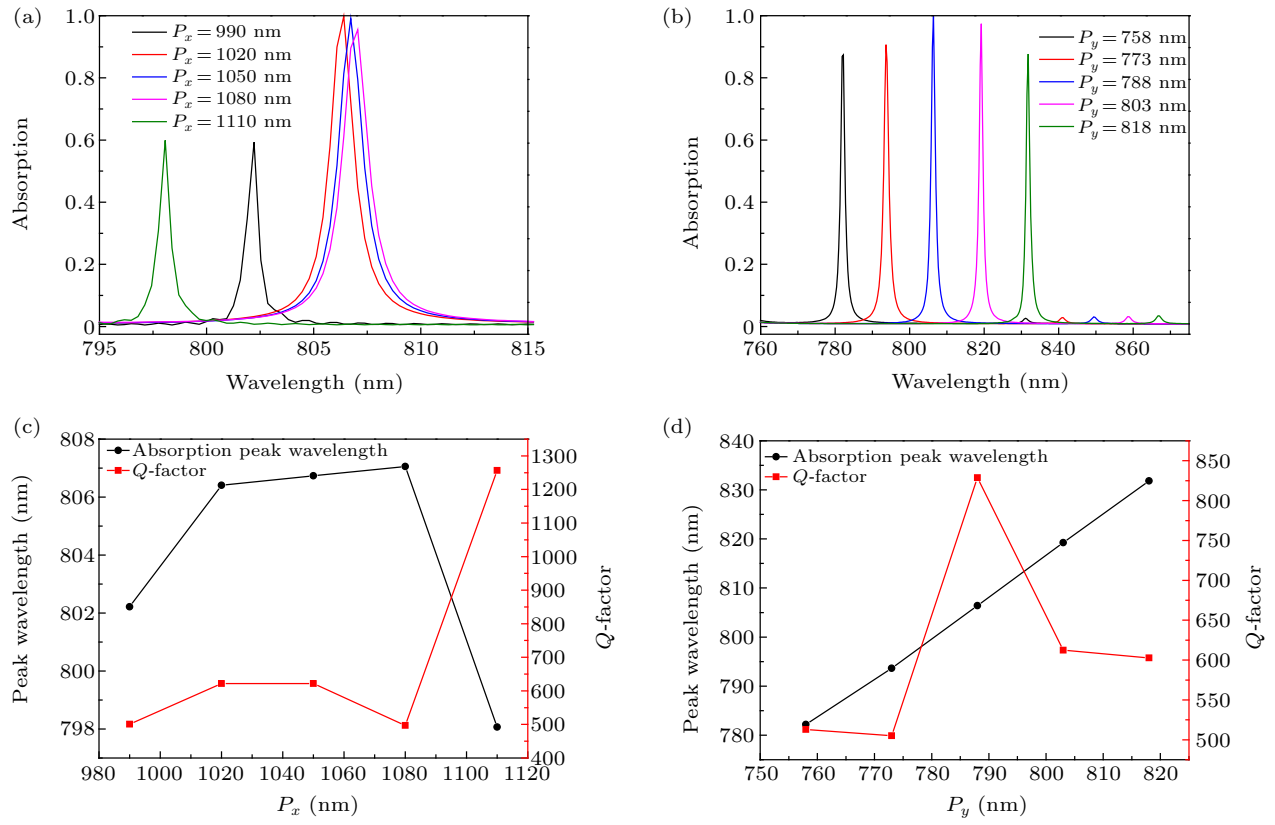


Fig. 3. (a), (b) Absorption spectra of different periods (P_x and P_y) based on a M-MoS_2 perfect absorber. (c), (d) The relationship between the change in period and the absorption peak wavelength and quality factor (keeping other parameters unchanged).

period and the leakage rate (γ_e), as shown in Figs. 3(a) and 3(b). In Fig. 3(a), when P_x changes from 990 nm to 1110 nm, the absorbance about the resonance absorption peak first increases and then decreases, and the spectrum first undergoes a red shift and then a blue shift. In Fig. 3(b), the absorption peak trend about P_y is consistent with that of P_x. When the period P_y increases, the value of the resonant absorption peak first increases and then declines, and there is a significant red shift in the position of the absorption peak. Meanwhile, the perfect absorption state is reached when $P_x = 1020$ nm and $P_y = 788$ nm. In the whole process, the structure goes through three states of uncoupling, critical coupling and overcoupling. After determining the other geometrical structure parameters of the absorber and reaching the critical coupling state, we then show the functional relationship between the periodic change and the absorption peak wavelength and Q-factor in Figs. 3(c) and 3(d). When P_x increases, the Q-factor $[= \lambda/\text{full width at half maximum (FWHM)}]$ of the system first increases, then decreases and finally increases again, while the absorption peak wavelength first increases and then decreases. Not only that, when P_y increases, the Q-factor of the structure first increases and then decreases. In summary, the maximum Q-factor is 1256.8 for the period $P_x = 1110$ nm, and the corresponding FWHM and resonance wavelength are 0.64 nm and 798.1 nm, respectively. The period $P_y = 788$ nm has a maximum Q-factor of 828.8, and the corresponding FWHM and resonance wavelengths are 0.97 nm and 806.41 nm, respectively. The superiority of the designed system compared with previous work is in the better sensing performance of the absorber (Table 1).[23–27]

Table 1. Contrast with uniform type absorbers.

Reference	Wavelength (nm)	FWHM (nm)	Q-factor
[23]	662	11.5	57.57
[24]	1500	20	75
[25]	679.2	8.72	77.89
[26]	663	11.35	58.32
[27]	661	9	73
Present work	798.1	0.64	1256.8

4. Conclusion

In general, we have obtained a perfect absorber with a M-MoS_2 structure. Meanwhile, the absorption characteristics simulated by the finite difference time domain method show that the absorption rate of the proposed MoS_2-based absorber at $\lambda = 806.41$ nm is as high as 99.8%. Our work also confirms, from both theoretical calculations and numerical simulations, that the reason for the perfect absorption of the ultranarrow band of M-MoS_2 is the strong limitation of the electromagnetic field by the critical coupling theory with guided resonance and suppression of the loss caused by reflection and transmission in the porous medium. By changing the structural parameters, the absorption spectrum can be moved in a wider wavelength range. At the same time, we also find that the maximum Q-factor of the structure is 1256.8 and the corresponding FWHM is 0.64 nm. Therefore, our research results may have important significance in the application of MoS_2-based photodetectors, optical switches, modulators and many other photonic and optoelectronic devices.

Acknowledgments

Project supported by the National Natural Science Foundation of China (Grant Nos. 11604311, 61705204, and 21506257), the Scientific Research Fund of SiChuan Provincial Science and Technology Department, China (Grant Nos. 2020YJ0137 and 2020YFG0467), the National Defense Science and Technology Innovation Special Zone Project of China (Grant No. 19-163-21-TS-001-067-01), and the College Students's Innovation and Entrepreneurship Training Program (Grant No. S202110619065).

References

[1] Smith D R, Padilla W J, Vier D C, Nemat-Nasser S C and Schultz S 2000 *Phys. Rev. Lett.* **84** 4184
[2] Li Z Y, Yi Y T, Xu D Y, Yang H, Yi Z, Chen X F, Yi Y G, Zhang J G and Wu P H 2021 *Chin. Phys. B* **30** 098102
[3] Deng Y, Cao G T, Yang H, Zhou X Q and Wu Y W 2018 *Plasmonics* **13** 345
[4] Landy N I, Sajuyigbe S, Mock J J, Smith D R and Padilla W J 2008 *Phys. Rev. Lett.* **100** 207402
[5] Zhang M D, Xu S, Hou X Y, Gu Y D, Zhang F, Xia T L, Ren Z A, Chen G F, Hao N and Shan L 2021 *Chin. Phys. B* **30** 017304
[6] Li Y F, Shi Q Z, Li Y, Song X J, Liu C C, Ta D and Wang W 2021 *Chin. Phys. B* **30** 014302
[7] Su J, Yang H, Xu Y, Tang Y, Yi Z, Zheng F S, Zhao F, Liu L, Wu P H and Li H L 2021 *Coatings* **11** 748
[8] Huang J, GuoL W, Lu W, ZhangY H, Shi Z, JiaY P, Li Z L, Yang J W, Chen H X, Mei Z X and Chen X L 2016 *Chin. Phys. B* **25** 067205
[9] Yi Z, Li J K, Lin J C, Qin F, Chen X F, Yao W T, Liu Z M, Cheng S B, Wu P H and Li H L 2020 *Nanoscale* **12** 23077
[10] Geim A K and Grigorieva I V 2013 *Nature* **499** 419
[11] Jiang L Y, Yi Y T, Yi Z, Yang H, Li Z Y, S J, Zhou Z G, Chen X F and Yi Y G 2021 *Acta Phys. Sin.* **70** 128101 (in Chinese)
[12] Chen Z H, Chen H, Yin J K, Zhang R Y, Jile H, Xu D Y, Yi Z, Zhou Z G, Cai S S and Yan P G 2021 *Diam. Relat. Mater.* **116** 108393
[13] Luo X, Liu Z M, Cheng Z Q, Liu J P, Lin Q and Wang L L 2018 *Opt. Express* **26** 33918
[14] Janisch C, Song H, Zhou C, Lin Z, Elías A L, Ji D and Liu Z 2016 *2D Mater.* **3** 025017
[15] Liu J T, Wang T B, Li X J and Liu N H 2014 *J. Appl. Phys.* **115** 193511
[16] Li Y, Chernikov A, Zhang X, Rigosi A, Hill H M, van der Zande A M and Heinz T F 2014 *Phys. Rev. B* **90** 205422
[17] Liu N, Liu H, Zhu S N and Giessen H 2009 *Nat. Photon.* **3** 157
[18] Deng Y, Cao G, Wu Y, Zhou X and Liao W 2015 *Plasmonics* **10** 1537
[19] Qi Y P, Zhang B H, Ding J H, Zhang T, Wang X X and Yi Z 2021 *Chin. Phys. B* **30** 024211
[20] Jiang L Y, Yuan C, Li Z Y, Su J, Yi Z, Yao W T, Wu P H, Liu Z M, Cheng S B and Pan M 2021 *Diam. Relat. Mater.* **111** 108227
[21] Cao G, Li H, Deng Y, Zhan S, He Z and Li B 2014 *Plasmonics* **9** 1163
[22] Chen Z H, Chen H, Jile H, Xu D Y, Yi Z, Lei Y L, Chen X F, Zhou Z G, Cai S S and Li G F 2021 *Diam. Relat. Mater.* **115** 108374
[23] Lu H, Gan X, Mao D, Fan Y, Yang D and Zhao J 2017 *Opt. Express* **25** 21630
[24] Guo C, Zhu Z, Yuan X, Ye W, Liu K, Zhang J, Xu Wei and Qin S 2016 *Adv. Opt. Mater.* **4** 1955
[25] Li H, Qin M, Wang L, Zhai X, Ren R and Hu J 2017 *Opt. Express* **25** 31612
[26] Cao J T, Yang G F, Gu Y, Fang X D, Lu N Y, Hua B and Yan X M 2019 *Mater. Res. Express* **6** 015050
[27] Piper J R, Liu V and Fan S 2014 *Appl. Phys. Lett.* **104** 251110